Nanoscale

ROYAL SOCIETY OF CHEMISTRY

PAPER

View Article Online
View Journal | View Issue

Cite this: *Nanoscale*, 2022, **14**, 1187

Browning of white adipocytes by gold nanocluster mediated electromagnetic induction heating hyperthermia†

Tiantian Xue,‡ Hejie Xu,‡ Yanhui Du, Jialuo Ding, Yu Su and Zhenkun Lin *

Browning of white adipose tissue (WAT) is becoming an attractive therapeutic target for obesity. Great efforts have been made to develop effective approaches to induce browning. Unfortunately, the current methods suffer from a series of disadvantages, such as low efficiency, unsatisfactory stability, and side effects. Herein, we report a new approach to induce browning of 3T3-L1 white adipocytes based on electromagnetic induction heating (EIH) hyperthermia. In particular, adipocyte-targeting aptamer modified gold nanoclusters (Apt-AuNCs) were employed as the mediators of EIH. Apt-AuNCs had good biocompatibility and excellent targeting performance with white adipocytes. After Apt-AuNCs/EIH treatment, adipocytes with characteristic multilocular and small lipid droplets increased, and the content of triglycerides reduced effectively. Apt-AuNCs/EIH treatment also significantly increased the mitochondrial activity in adipocytes. Meanwhile, the mRNA levels of key genes that are involved in browning, for example UCP1, PRDM16, PPARγ, and PGC-1α, were upregulated. Finally, the induction mechanism of Apt-AuNCs/EIH on browning of white adipocytes was explained by the synergistic effects of EIH hyperthermia and pharmacological action of AuNCs. To the best of our knowledge, this is the first attempt on induction of browning by metal nanocluster-mediated EIH hyperthermia, thus providing an interesting and efficient channel for obesity treatment.

Received 3rd November 2021,
Accepted 12th December 2021

DOI: 10.1039/d1nr07263c

rsc.li/nanoscale

1. Introduction

Obesity has become a global epidemic,[1] which is seriously threatening to human health. It has been confirmed that obesity is a risk factor for a series of chronic diseases, such as type 2 diabetes,[2] cardiovascular diseases,[3] hypertension,[4] and cancer.[5] Conventional approaches for treatment of obesity mainly include lifestyle modification, pharmacotherapy, and surgery. Unfortunately, these approaches usually suffer failure in practice, owing to low success rate, adverse side effects, or high risks.[6–8] Consequently, scientists have been pursuing new anti-obesity strategies.

Adipose tissues are traditionally categorized into two types according to the function and morphology, white adipose tissue (WAT) and brown adipose tissue (BAT). Recently, scientists surprisingly discovered that, in response to appropriate stimuli, WAT from certain depots would present a BAT phenotype such as multilocular lipid droplets, multiple mitochondria, and high expression of uncoupling protein 1 (UCP1).[9] These inducible or recruitable brown-like adipocytes are termed beige adipocytes, and correspondingly this process is known as browning.[10]

Obviously, the discovery of browning points to a new way for anti-obesity treatment. The beige adipocytes from the browning of WAT have similar characteristics to brown adipose tissue, including adaptive thermogenesis and energy expenditure.[11] Thus, beige adipocytes, that is browning of WAT, is becoming an attractive therapeutic target for obesity and obesity-related diseases.[12]

The current methods for induction of browning can be classified into two approaches, physiological stimuli (*e.g.*, cold exposure and exercise) and pharmacological treatment.[13] Cold exposure can upregulate UCP1 expression, induce the reconstruction of subcutaneous white adipose tissue, and promote the differentiation of beige adipose tissue.[14] More and more evidence supports that cold exposure induced browning is a complex process that is regulated by various factors.[15–18] Exercise can induce browning by promoting a series of transcriptional regulators such as PGC-1α, as well as hormones such as Irisin and FGF21.[19–23] Meanwhile, pharmacological treatment induced browning has been significantly developed in the last decade, including through hormones,[24–26]

Research Center of Basic Medicine, The Second Affiliated Hospital of Wenzhou Medical University, Wenzhou 325027, China. E-mail: zklin@wmu.edu.cn

†Electronic supplementary information (ESI) available. See DOI: 10.1039/d1nr07263c

‡These authors contributed to this work equally.

nutrients,[27–29] and microRNAs.[30,31] Unfortunately, in these traditional strategies for the induction of browning, a series of disadvantages emerged. Physiological stimuli sometimes had low efficiency and unsatisfactory stability,[27,32] while pharmacological treatment leads to different degrees of side effects.[27] Furthermore, the mechanisms in induction of browning, both for physiological stimuli and pharmacological treatment, are unclear and even inconsistent. Therefore, it is urgent to seek a new approach for the induction of browning to achieve good stability and high precision.

In this work, we present a novel approach to induce browning of white adipocytes by gold nanocluster (AuNC) mediated electromagnetic induction heating (EIH) hyperthermia, as shown in Fig. 1. AuNCs, characterized by a core–shell structure and an ultrasmall size (usually <2 nm), have recently emerged as a novel class of gold nanoparticles.[33,34] Benefiting from their unique physical and chemical properties such as ultrasmall size, good biocompatibility, and low toxicity, AuNCs showed promising potential in biomedical applications.[35–38] We herein modify AuNCs with a white adipocyte-targeting aptamer (termed as Apt-AuNCs), that were further employed as mediators of EIH in inducing browning. To the best of our knowledge, this is the first attempt on induction of browning by metal nanocluster mediated EIH hyperthermia, thus providing an interesting and efficient channel for obesity treatment.

2. Experimental section

2.1 Materials

Hydrogen tetrachloroaurate(III) hydrate ($HAuCl_4 \cdot 3H_2O$), sodium borohydride ($NaBH_4$), 6-mercaptohexanoic acid (MHA), 3-isobutyl-1-methylxanthine (IBMX) and oil red O were purchased from Sigma-Aldrich. Sodium hydroxide (NaOH), potassium hydroxide (KOH), *n*-heptane and isopropanol were purchased from Sinopharm Chemical Reagent Co., Ltd. MA-33 aptamer, random ssDNA sequences, and primers (5′-3′) used for qPCR were purchased from Shanghai Sangon Biotechnology Co., Ltd. Mito-Tracker Red CMXRos and Hoechst 33342 were purchased from Beyotime. Iron fortified bovine serum (IF-BS) was purchased from ScienCell. High glucose Dulbecco's Modified Eagle's Medium (DMEM) was purchased from Shanghai Zhongqiaoxinzhou Biotechnology Co., Ltd. Dexamethasone (DEX), insulin, 4% paraformaldehyde, and penicillin–streptomycin were purchased from Solarbio. 0.25% trypsin-EDTA (1×) was purchased from Gibco. Cell proliferation kit I was purchased from Roche. UNIQ-10 column Trizol total RNA extraction kit was purchased from Shanghai Sangon Biotechnology Co., Ltd. Triglyceride (TG) content assay kit was purchased from Solarbio. TB Green Fast qPCR mix and PrimeScript RT reagent kit were purchased from Takara. Ultrapure Millipore water (18.2 MΩ) was used throughout the experiment.

2.2 Synthesis of Apt-AuNCs

The synthesis of Apt-AuNCs was carried out by a modification of the NaOH-mediated $NaBH_4$ reduction method.[39] In particular, MA-33 aptamer was added as a co-ligand to achieve good targeting performance towards 3T3-L1 white adipocytes.[40] 2.35 mL of H_2O, 0.25 mL of $HAuCl_4$ (20 mM), 2 mL of MHA (5 mM), and MA-33 aptamer (5 OD) were gently mixed together for 30 minutes, then 0.3 mL of NaOH solution (1 M) and 0.1 mL of $NaBH_4$ solution (0.1 M, $NaBH_4$ powder dissolved in NaOH solution) were added, followed by stirring (300 rpm) at room temperature (RT) for 3 h. The crude product was further purified by centrifugation (4000 rpm) coupled with an ultrafiltration centrifuge tube (3 kDa) for 60 minutes. In addition, FAM (green fluorescence)-labeled aptamer as a fluorescent tracer was used in the synthesis of Apt-AuNCs for a particular experiment, such as the evaluation of the binding efficiency of the aptamer on AuNCs and the targeting performance of Apt-AuNCs on 3T3-L1 white adipocytes.

2.3 Characterization

Transmission electron microscopy (TEM) was performed on a JEM 2100F with an acceleration voltage of 200 kV. UV-Vis absorption spectra were obtained on a MAPADA UV-6100s spectrometer. Fluorescence spectra were obtained on a Lengguang F96 Pro fluorescence spectrometer.

2.4 Cell culture and differentiation

3T3-L1 preadipocytes were obtained from Shanghai Zhongqiaoxinzhou Biotechnology Co., Ltd. Preadipocytes were maintained in DMEM with 10% IF-BS and 1% penicillin–strep-

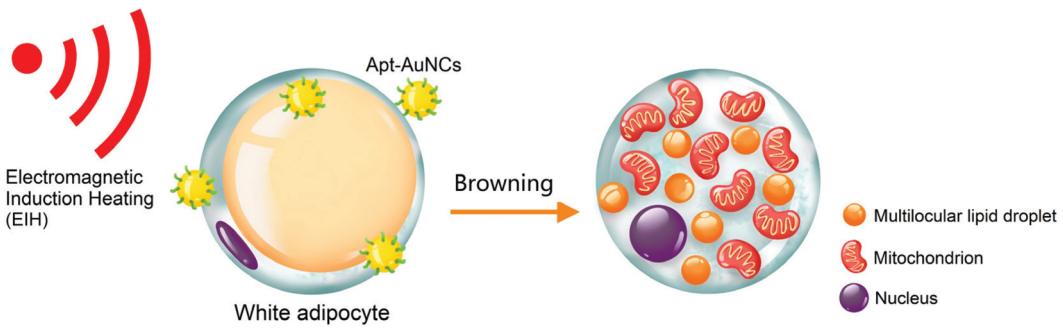

Fig. 1 Schematic illustration of browning of white adipocytes by gold nanocluster mediated electromagnetic induction heating hyperthermia.

tomycin (termed the complete medium) at 37 °C, in a humidified atmosphere containing 5% CO_2. Until confluence, differentiation of 3T3-L1 preadipocytes was induced by incubation with the complete medium containing 0.5 mM IBMX, 0.5 μM DEX, and 2 μg mL^{-1} insulin for two days. Then, the medium was replaced with the complete medium containing 2 μg mL^{-1} insulin for two days. Finally, the complete medium was changed every two days until full differentiation was achieved, and 3T3-L1 white adipocytes were obtained.

2.5 Apt-AuNC targeting of white adipocytes

AuNCs were modified with MA-33 aptamer to realize the specific binding to white adipocytes.[40] Thus, a FAM-labeled aptamer was employed for fluorescence tracing in this experiment to evaluate the targeting performance of Apt-AuNCs. Furthermore, two random ssDNAs, instead of MA-33 aptamer, were respectively used in the modification of AuNCs. Information on the MA-33 aptamer and two random ssDNAs is listed in Table S1.† 3T3-L1 white adipocytes were incubated with Apt-AuNCs or random ssDNA modified AuNCs for 2 h, and then stained with Hoechst 33342 (cell nuclei) at RT for 5 minutes. The fluorescence imaging was performed on a confocal laser scanning microscope (Leica TCS sp8).

2.6 Cell proliferation assay

MTT assay was employed to evaluate the biocompatibility of Apt-AuNCs. 3T3-L1 preadipocytes were seeded in a 96-well plate, cultured and differentiated for 2, 4, 6, 8 days respectively, followed by incubation with the complete medium including Apt-AuNCs for 48 h. The concentration of Apt-AuNCs was 5, 25, and 50 μg mL^{-1} respectively. Finally, the viability of adipocytes was tested by MTT assay.

2.7 Apt-AuNCs/EIH treatment of white adipocytes

For the Apt-AuNCs/EIH group, 3T3-L1 white adipocytes were firstly cultured in the complete medium including Apt-AuNCs (25 μg mL^{-1}) for 24 h, and then made to undergo EIH treatment as follows. High-frequency alternating magnetic field (AMF) was induced inside the strap coil of the EIH instrument (Shenzhen Shuangping Power Supply Technologies Co., Ltd) when high-frequency alternating current was passed. The cell culture dish was located in the areas of AMF, and then the Apt-AuNCs generated and released heat (Joule heat). The power of the EIH instrument in this experiment was 1.5 kW, and the treatment time was 30 minutes. It was observed that the temperature of the culture medium with Apt-AuNCs increased slowly and finally reached approximately 43 °C. After EIH treatment, the adipocytes were collected for subsequent tests. In addition, 3T3-L1 white adipocytes that were cultured in an identical medium but without EIH treatment were termed the Apt-AuNCs group, while those with identical EIH treatment but cultured in the medium without Apt-AuNCs were termed the EIH group.

2.8 Oil Red O staining experiment

TG in adipocytes was stained by Oil Red O for observation of the intracellular lipid droplets. Adipocytes were washed with PBS (pH 7.4), and then fixed with 4% paraformaldehyde for 40 minutes at RT. After that, adipocytes were washed in order with ultrapure Millipore water and 60% isopropanol, followed by staining with Oil Red O for 50 minutes at RT. Finally, photographs were taken under a bright field using an inverted microscope (Nikon, Eclipse Ti).

2.9 Triglyceride detection

A TG content assay kit was used to determine the content of TG in adipocytes. The adipocytes were firstly washed with PBS followed by adding 1 mL of *n*-heptane/isopropanol solution (1 : 1), and then were ultrasonically crushed and centrifuged to collect the supernatant. After the operation following the instruction of the TG content assay kit, the obtained product was transferred to a 96-well plate. Finally, the absorbance value was obtained by the enzyme-labeling instrument to calculate the content of TG.

2.10 Mitochondrial staining experiment

Firstly, 50 μg of Mito-Tracker Red CMXRos powder was dissolved into 470 μL of anhydrous DMSO, thus Mito-Tracker Red CMXRos stock solution (200 μM) was obtained. Prior to use, the staining solution was prepared by diluting the stock solution with the culture medium (1 : 1000) and incubation at 37 °C. Secondly, the culture medium of adipocytes was removed, followed by adding the staining solution that was prepared above and incubation at 37 °C for 25 minutes. After removing the staining solution, the adipocytes were fixed with 4% paraformaldehyde for 20 minutes at RT. Finally, the cell nuclei were stained with Hoechst 33342 at RT for 5 minutes. The fluorescence imaging was carried out on a confocal laser scanning microscope (Leica TCS sp8).

2.11 Quantitative real-time PCR analysis (qRT-PCR)

Total cellular RNA was extracted using a UNIQ-10 column Trizol Total RNA extraction kit, and the concentration of RNA was determined using a NanoDrop 2000 instrument. The extracted RNA was reverse-transcribed into cDNA using the PrimeScript RT reagent kit, and cDNA was used to perform real-time PCR using the TB Green Fast qPCR mix in a Roche LightCycler 480 Real-Time PCR system. Finally, the mRNA levels of target genes were quantified relative to GADPH. Information for the primer sequences used in qRT-PCR is listed in Table S2.†

2.12 Statistical analysis

Student's *t* test was used to determine the significance between two groups with GraphPad Prism 8. A p value of <0.05 was considered to be statistically significant, and is presented as *($p < 0.05$), **($p < 0.01$), or ***($p < 0.001$). Errors bars plotted on graphs are presented as the mean ± SEM.

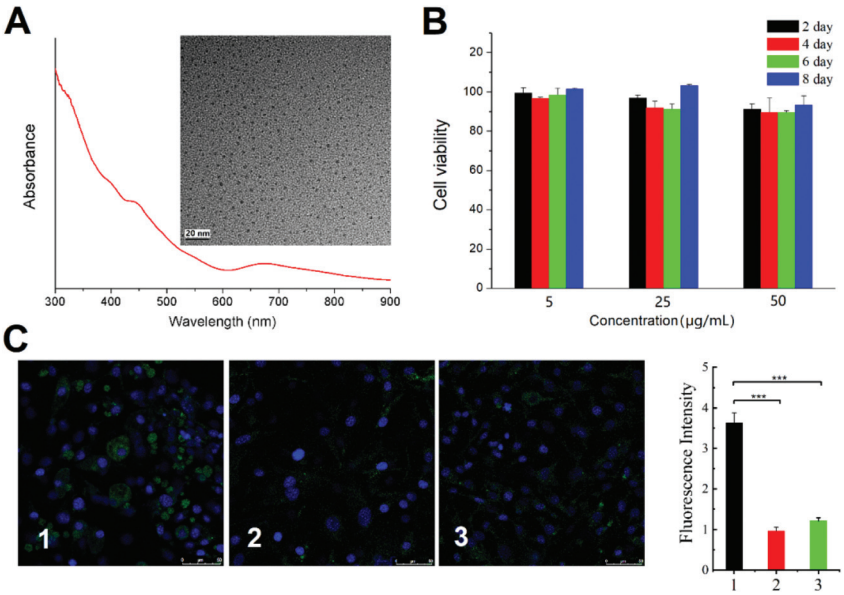

Fig. 2 (A) UV/Vis absorption of Apt-AuNCs (Inset: TEM image); (B) viability of adipocytes treated with Apt-AuNCs; (C) targeting capability towards 3T3-L1 white adipocytes (1: AuNCs modified with MA-33 aptamer, that is Apt-AuNCs; 2 and 3: AuNCs modified with two random ssDNA. The cell nuclei were stained with blue fluorescence Hoechst 33342, and aptamer was labeled with green fluorescence FAM).

3. Results and discussion

3.1 Synthesis and characterization of Apt-AuNCs

To achieve good targeting performance toward 3T3-L1 white adipocytes, the MA-33 aptamer and MHA were employed as the co-ligands in the synthesis of atomically precise gold nanoclusters (Au_{25}). It has been reported that the MA-33 aptamer (ssDNA) had good specificity for 3T3-L1 white adipocytes.[40] The UV/Vis spectra of the as-synthesized aptamer modified gold nanoclusters (Apt-AuNCs) are shown in Fig. 2A. Apt-AuNCs exhibit three clear absorption peaks at 400 nm, 450 nm, and 670 nm, which are in accordance with the previous reported thiolate Au_{25} nanoclusters.[41] The TEM image showed that Apt-AuNCs possessed highly uniform size (~2 nm) without aggregation. These results revealed that the surface modification by employing an aptamer as the co-ligand did not affect the structure of Au_{25} nanoclusters. Meanwhile, fluorescence spectra for the purified Apt-AuNCs (aptamer labeled with FAM) and filtrate from centrifugation affirmed that aptamer modification of AuNCs was successfully achieved as shown in Fig. S1.†

An MTT test was carried out to evaluate the biocompatibility of Apt-AuNCs toward adipocytes *in vitro*. As shown in Fig. 2B, after treatment with 5, 25, or 50 μg mL^{-1} Apt-AuNCs for 2, 4, 6, or 8 days, no obvious effect on the cell viability was observed. This result revealed that Apt-AuNCs had good biocompatibility and low cytotoxicity to adipocytes.

To study the targeting performance of Apt-AuNCs toward 3T3-L1 white adipocytes, a FAM-labeled aptamer was used for fluorescence tracing. Meanwhile, two random ssDNAs instead of the MA-33 aptamer were respectively used to modify AuNCs, which were adopted as the controls. As shown in Fig. 2C, Apt-AuNCs (with MA-33 aptamer) exhibited excellent binding capability toward 3T3-L1 white adipocytes. The quantitative analysis based on the fluorescence intensity showed that the binding efficiency of Apt-AuNCs was significantly higher than that of the controls by 3–4 times. Evidently, the good targeting performance of Apt-AuNCs was derived from the MA-33 aptamer. Kim and colleagues have demonstrated that MA-33 can specifically recognize mature 3T3-L1 white adipocytes with an equilibrium dissociation constant of 142.9 nM and did not bind to preadipocytes or other cell lines.[40]

3.2 Apt-AuNC mediated EIH hyperthermia induces browning of white adipocytes

Apt-AuNCs were employed as the mediators of EIH to induce the browning of white adipocytes in this study. Firstly, the distribution and morphology of intracellular lipid droplets in adipocytes were studied through Oil Red O staining. As shown in Fig. 3A, adipocytes in the control group mostly possessed a monolocular and big lipid droplet, which was a typical characteristic of white adipocytes. After treatment with Apt-AuNCs, EIH, or Apt-AuNCs/EIH, the ratio of adipocytes with big monolocular lipid droplets decreased at different degrees, while some adipocytes with the features of brown/beige adipocytes emerged, that is multilocular and small lipid droplets. Furthermore, the contents of TG in adipocytes for different groups were detected as shown in Fig. 3B, in accordance with the results from Oil Red O staining. The content of TG in Apt-AuNCs/EIH group was much lower than in the control group, EIH group, or Apt-AuNCs/EIH group, revealing that Apt-AuNCs/EIH treatment can effectively reduce the content of TG in adipocytes.

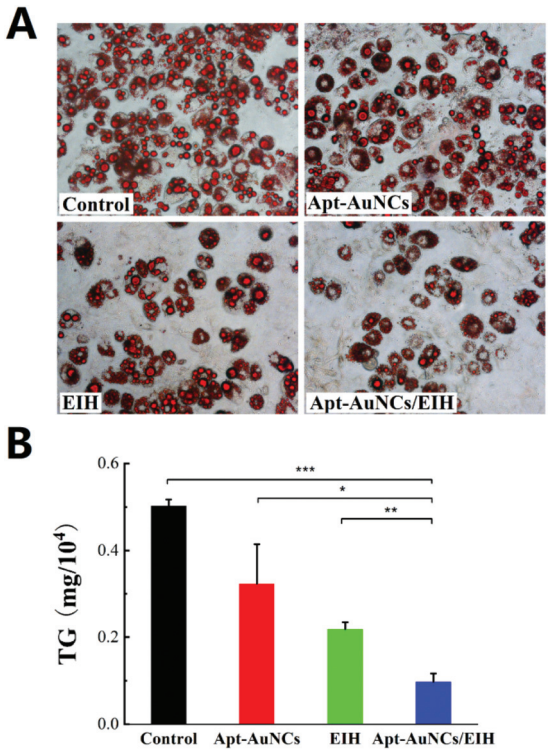

Fig. 3 (A) Distribution and morphology of intracellular lipid droplets in adipocytes by Oil Red O staining; (B) content of triglyceride (TG).

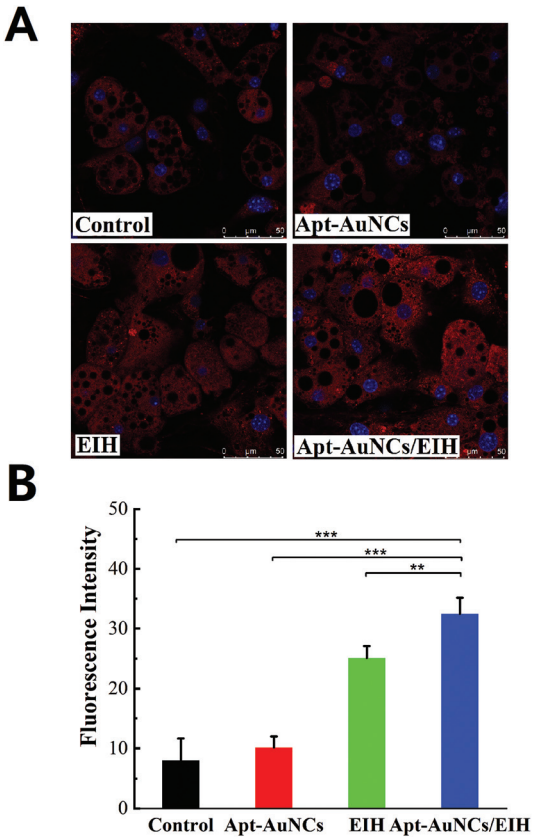

Fig. 4 (A) Images of mitochondria in adipocytes (the cell nuclei and mitochondria were stained with Hoechst 33342 (blue) and MitoTracker red CMXRos, respectively); (B) quantitative results of mitochondria activity based on the fluorescence intensity.

Brown/beige adipocytes usually have multiple mitochondria and high thermogenesis activity compared with white adipocytes.[9,11,41–43] Therefore, mitochondrial activity is an important indicator for browning of white adipocytes. As shown in Fig. 4, the mitochondrial activity in adipocytes after Apt-AuNCs/EIH treatment increased significantly by approximately four times, based on the fluorescence intensity of MitoTracker Red CMXRos (mitochondrial-specific fluorescence probe). It was interesting that EIH treatment also obviously increased the mitochondrial activity of adipocytes, revealing that EIH also had an inductive effect on browning of white adipocytes.

BAT plays a role of non-shivering thermogenesis and therefore maintains the energy balance of the body[44,45] through the characteristic protein UCP1 by uncoupling electron transport from adenosine triphosphate (ATP) production.[46] The expression of UCP1 was considered the most distinguishing feature of BAT.[47] Recent studies have found that beige adipocytes presented a series of characteristics that are similar to brown adipocytes, including the increased expression of UCP1.[9,48] Therefore, UCP1 is considered the most important biomarker for browning of white adipocytes. As shown in Fig. 5, the mRNA expression of UCP1 in the control group (3T3-L1 white adipocytes) was extremely low as expected. Apt-AuNCs/EIH treatment significantly increased the mRNA expression of UCP1 by 40 times, compared with that in the control group.

PRDM16, PPARγ, and PGC-1α are the most studied transcription factors that regulate the browning of white adipocytes.[10] As shown in Fig. 5, Apt-AuNCs/EIH treatment significantly increased the mRNA expression of PRDM16 by two orders of magnitude. Meanwhile, the mRNA expression of PPARγ and PGC-1α in Apt-AuNCs/EIH group was respectively two and three times higher than that in the control group.

Apt-AuNCs/EIH treatment significantly increased the mRNA expression of Cox8b by 10 times, while Apt-AuNC treatment or EIH treatment resulted in little change, as shown in Fig. 5. It was reported that PRDM16 expression can increase the mRNA levels of many genes that are involved in mitochondrial oxidative phosphorylation, including Cox8b, a specific mitochondrial gene of BAT.[49] This conclusion was well supported by the experimental results in this study, as both PRDM16 and Cox8b in adipocytes gained significantly increased mRNA expression after Apt-AuNCs/EIH treatment. Similarly, Apt-AuNCs/EIH treatment significantly increased the mRNA expression of CEBPα and CEBPβ respectively by 11 and 8 times. The mRNA expression of CIDEA in the Apt-AuNCs/EIH group was two times higher than that in the control group.

Different from most genes discussed above, the mRNA expression of FGF21 was only slightly changed as shown in Fig. 5, revealing that FGF21 in 3T3-L1 white adipocytes was comparatively insensitive to Apt-AuNCs/EIH treatment. It has

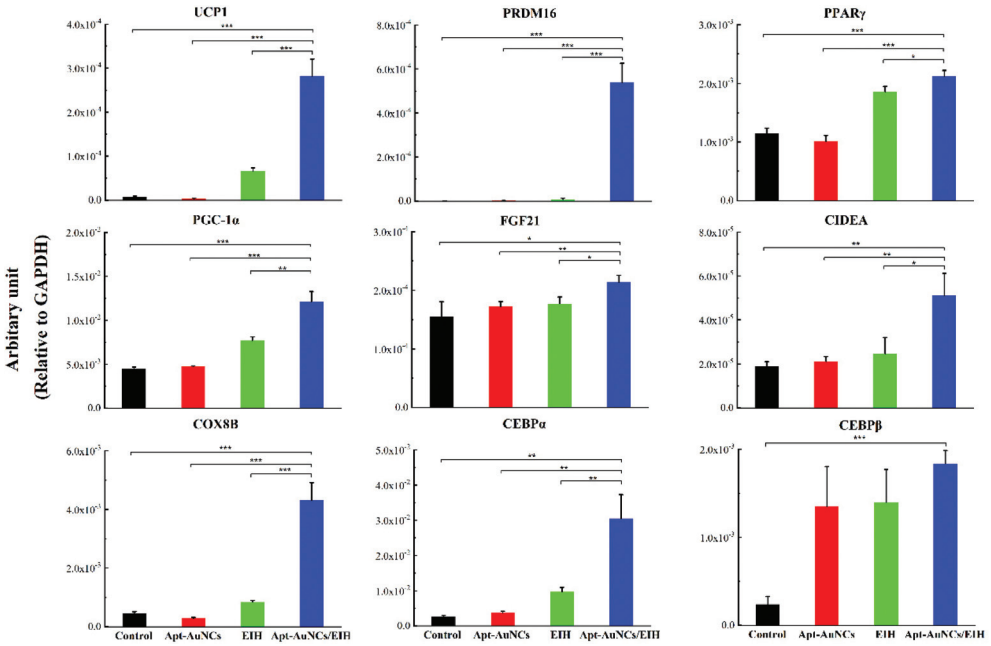

Fig. 5 mRNA expression of UCP1, PRDM16, PPARγ, PGC-1α, FGF21, CIDEA, COX8B, CEBPα, and CEBPβ in adipocytes.

been reported that cold stimulation and a β3-adrenoceptor agonist can induce the mRNA expression of FGF21.[50] This result indicated that the mechanism of browning by Apt-AuNCs/EIH treatment was possibly different from that by cold stimulation or a β3-adrenoceptor agonist.

3.3 Synergistic effects of EIH hyperthermia and pharmacological action of AuNCs potentially contribute to the browning of white adipocytes

Hyperthermia is currently considered an innovative therapeutic approach due to the high efficiency and reduced side effects,[51,52] and magnetic nanoparticles are the most frequently used mediators.[53,54] Recently, Marinozzi *et al.* found that superparamagnetic iron oxide nanoparticle (SPION) mediated hyperthermia can induce controlled lipolysis in 3T3-L1 adipocytes, thus providing a novel and safe therapeutic approach against obesity.[55] In the present study, Apt-AuNCs were employed as the mediators of heating. Although equally subjected to AMF, the heating mechanism of Apt-AuNCs was different from that of magnetic nanomaterials. The heat generation of magnetic nanomaterials in AMF originates from the Brownian–Néel relaxation and hysteresis losses.[56–58] As for Apt-AuNCs, the generated heat was actually Joule heat as AMF can produce alternating current, which was also termed EIH. In the present study, owing to the ultrasmall size (~2 nm), Apt-AuNCs/EIH produced a very small amount of heat, which may modulate the microenvironment of the adipocytes and then induce the browning. It was observed that EIH treatment (in the absent of Apt-AuNCs) also led to the browning of white adipocytes to a certain extent, as mentioned above. The culture medium of adipocytes (DMEM) contained a large number of metal ions and anions. When exposed to AMF, those metal ions and anions would generate heat, which further contributed to the induction of browning.

In addition, the potential pharmacological effect of Apt-AuNCs was also a primary cause to induce browning. As a special state of matter between metal atoms and metal nanoparticles,[59] metal nanoclusters have unique physical and chemical properties. Previous studies have demonstrated that, as a new type of chemotherapeutic agent, metal nanoclusters including AuNCs can realize good therapeutic efficacy.[60] It was supposed that EIH treatment enhanced the pharmacological effect of Apt-AuNCs and affected the physiology of adipocytes, which ultimately induced browning. In a previous study on hyperthermia treatment of adipocytes that adopted SPIONs as the heating mediators, no significant difference on the mRNA expression of key genes including PPARγ was observed.[55] However, in the present study, several key transcription factors that are involved in browning, for example PPARγ, PRDM16, and PGC-1α, were upregulated by Apt-AuNCs/EIH treatment as shown in Fig. 5. This result suggested that Apt-AuNCs not only acted as the heating mediators of hyperthermia like SPIONs but also played an important role in regulating the transcription factors of browning. However, more efforts should be made to explore the detailed pharmacology of AuNCs in browning of white adipocytes in the future.

In a word, Apt-AuNCs/EIH induced browning of white adipocytes possibly came from the synergistic effects of EIH hyperthermia and pharmacological action of AuNCs. When subjected to AMF, Apt-AuNCs were heated by EIH, which enhanced the pharmacological action of Apt-AuNCs. Changes in the microenvironment of adipocytes by EIH hyperthermia,

together with the enhanced pharmacological effect of Apt-AuNCs, led to the upregulation of key transcription factors and ultimately induced the browning of white adipocytes.

4. Conclusion

We developed a novel approach to induce browning of 3T3-L1 white adipocytes by Apt-AuNCs mediated EIH hyperthermia. Apt-AuNCs/EIH treatment can effectively induce the browning of white adipocytes, resulting in multilocular and small lipid droplets, reduced triglyceride content, and increased mitochondrial activity. Meanwhile, the mRNA levels of key genes that are involved in browning were upregulated. The induction mechanism was also discussed through the synergistic effects of EIH hyperthermia and pharmacological action of AuNCs. We realized the browning of white adipocytes by metal nanocluster mediated hyperthermia for the first time, presenting a new and promising way for obesity treatment.

Conflicts of interest

There are no conflicts of interest to declare.

Acknowledgements

This work was financially supported by the Wenzhou Science and Technology Plan Project (ZY2021012), the Zhejiang Basic Public Welfare Research Program (LGF19H030014), and the Zhejiang Medical Science and Technology Project (2021RC093).

References

1 GBD 2017 Diet Collaborators, *Lancet*, 2019, **393**, 1958–1972.
2 R. H. Eckel, S. E. Kahn, E. Ferrannini, A. B. Goldfine, D. M. Nathan, M. W. Schwartz, R. J. Smith and S. R. Smith, *J. Clin. Endocrinol. Metab.*, 2011, **96**, 1654–1663.
3 C. J. Lavie, R. V. Milani and H. O. Ventura, *J. Am. Coll. Cardiol.*, 2009, **53**, 1925–1932.
4 K. Narkiewicz, *Nephrol., Dial., Transplant.*, 2006, **21**, 264–267.
5 G. A. Bray, *J. Nutr.*, 2002, **132**, 3451s–3455s.
6 A. Ballinger and S. R. Peikin, *Eur. J. Pharmacol.*, 2002, **440**, 109–117.
7 R. F. Kushner, *Expert Opin. Pharmacother.*, 2008, **9**, 1339–1350.
8 D. Rucker, R. Padwal, S. K. Li, C. Curioni and D. C. Lau, *Br. Med. J.*, 2007, **335**, 1194–1199.
9 J. R. Brestoff and D. Artis, *Cell*, 2015, **161**, 146–160.
10 K. A. Lo and L. Sun, *Biosci. Rep.*, 2013, **33**, e00065.
11 J. Wu, P. Cohen and B. M. Spiegelman, *Genes Dev.*, 2013, **27**, 234–250.
12 F. Lizcano, *Int. J. Mol. Sci.*, 2019, **20**, 5058.
13 A. C. Lehnig, R. S. Dewal, L. A. Baer, K. M. Kitching, V. R. Munoz, P. J. Arts, D. A. Sindeldecker, F. J. May, H. Lauritzen, L. J. Goodyear and K. I. Stanford, *iScience*, 2019, **11**, 425–439.
14 J. Dempersmier, A. Sambeat, O. Gulyaeva, S. M. Paul, C. S. Hudak, H. F. Raposo, H. Y. Kwan, C. Kang, R. H. Wong and H. S. Sul, *Mol. Cell*, 2015, **57**, 235–246.
15 P. Lee, J. D. Linderman, S. Smith, R. J. Brychta, J. Wang, C. Idelson, R. M. Perron, C. D. Werner, G. Q. Phan, U. S. Kammula, E. Kebebew, K. Pacak, K. Y. Chen and F. S. Celi, *Cell Metab.*, 2014, **19**, 302–309.
16 F. Li, R. Wu, X. Cui, L. Zha, L. Yu, H. Shi and B. Xue, *J. Biol. Chem.*, 2016, **291**, 4523–4536.
17 S. Y. Shi, W. Zhang, C. T. Luk, T. Sivasubramaniyam, J. J. Brunt, S. A. Schroer, H. R. Desai, A. Majerski and M. Woo, *Diabetologia*, 2016, **59**, 187–196.
18 A. Fenzl, O. C. Kulterer, K. Spirk, G. Mitulović, R. Marculescu, M. Bilban, S. Baumgartner-Parzer, A. Kautzky-Willer, L. Kenner, J. Plutzky, L. Quadro and F. W. Kiefer, *Mol. Metab.*, 2020, **42**, 101088.
19 P. Boström, J. Wu, M. P. Jedrychowski, A. Korde, L. Ye, J. C. Lo, K. A. Rasbach, E. A. Boström, J. H. Choi, J. Z. Long, S. Kajimura, M. C. Zingaretti, B. F. Vind, H. Tu, S. Cinti, K. Højlund, S. P. Gygi and B. M. Spiegelman, *Nature*, 2012, **481**, 463–468.
20 F. M. Fisher, P. C. Chui, P. J. Antonellis, H. A. Bina, A. Kharitonenkov, J. S. Flier and E. Maratos-Flier, *Diabetes*, 2010, **59**, 2781–2789.
21 E. Hondares, M. Rosell, J. Díaz-Delfín, Y. Olmos, M. Monsalve, R. Iglesias, F. Villarroya and M. Giralt, *J. Biol. Chem.*, 2011, **286**, 43112–43122.
22 A. M. Gonzalez-Gil and L. Elizondo-Montemayor, *Nutrients*, 2020, **12**, 1899.
23 M. Khalafi, H. Mohebbi, M. E. Symonds, P. Karimi, A. Akbari, E. Tabari, M. Faridnia and K. Moghaddami, *Nutrients*, 2020, **12**, 925.
24 N. Zelcer and P. Tontonoz, *J. Clin. Invest.*, 2006, **116**, 607–614.
25 A. Rodríguez, S. Ezquerro, L. Méndez-Giménez, S. Becerril and G. Frühbeck, *Am. J. Physiol. Endocrinol. Metab.*, 2015, **309**, E691–E714.
26 M. López, L. Varela, M. J. Vázquez, S. Rodríguez-Cuenca, C. R. González, V. R. Velagapudi, D. A. Morgan, E. Schoenmakers, K. Agassandian, R. Lage, P. B. Martínez de Morentin, S. Tovar, R. Nogueiras, D. Carling, C. Lelliott, R. Gallego, M. Oresic, K. Chatterjee, A. K. Saha, K. Rahmouni, C. Diéguez and A. Vidal-Puig, *Nat. Med.*, 2010, **16**, 1001–1008.
27 Z. X. Xie, S. F. Xia, Y. Qiao, Y. H. Shi and G. W. Le, *J. Anim. Physiol. Anim. Nutr.*, 2015, **99**, 492–500.
28 P. Baskaran, V. Krishnan, J. Ren and B. Thyagarajan, *Br. J. Pharmacol.*, 2016, **173**, 2369–2389.
29 L. D. Roberts, P. Boström, J. F. O'Sullivan, R. T. Schinzel, G. D. Lewis, A. Dejam, Y.-K. Lee, M. J. Palma, S. Calhoun, A. Georgiadi, M.-H. Chen, V. S. Ramachandran, M. G. Larson, C. Bouchard, T. Rankinen, A. L. Souza,

C. B. Clish, T. J. Wang, J. L. Estall, A. A. Soukas, C. A. Cowan, B. M. Spiegelman and R. E. Gerszten, *Cell Metab.*, 2014, **19**, 96–108.
30 Z. Zheng, X. Liu, Q. Zhao, L. Zhang, C. Li and Y. Xue, *Int. J. Endocrinol.*, 2014, **2014**, 530636.
31 S. Gharanei, K. Shabir, J. E. Brown, M. O. Weickert, T. M. Barber, I. Kyrou and H. S. Randeva, *Cells*, 2020, **9**, 2489.
32 F. Norheim, T. M. Langleite, M. Hjorth, T. Holen, A. Kielland, H. K. Stadheim, H. L. Gulseth, K. I. Birkeland, J. Jensen and C. A. Drevon, *FEBS J.*, 2014, **281**, 739–749.
33 H. Xu and K. S. Suslick, *Adv. Mater.*, 2010, **22**, 1078–1082.
34 J. Zheng, P. R. Nicovich and R. M. Dickson, *Annu. Rev. Phys. Chem.*, 2007, **58**, 409–431.
35 Q. Li, Q. Yuan, M. Zhao, Y. Yao, L. Gao, R. Liu, Y. Wang, Y. Gong, F. Gao and X. Gao, *Sci. Bull.*, 2017, **62**, 537–545.
36 P. Liu, W. Yang, L. Shi, H. Zhang, Y. Xu, P. Wang, G. Zhang, W. R. Chen, B. Zhang and X. Wang, *J. Mater. Chem. B*, 2019, **7**, 6924–6933.
37 S. K. Katla, J. Zhang, E. Castro, R. A. Bernal and X. Li, *ACS Appl. Mater. Interfaces*, 2018, **10**, 75–82.
38 R. Han, M. Zhao, Z. Wang, H. Liu, S. Zhu, L. Huang, Y. Wang, L. Wang, Y. Hong, Y. Sha and Y. Jiang, *ACS Nano*, 2020, **14**, 9532–9544.
39 X. Yuan, B. Zhang, Z. Luo, Q. Yao, D. T. Leong, N. Yan and J. Xie, *Angew. Chem., Int. Ed.*, 2014, **53**, 4623–4627.
40 E. Y. Kim, J. W. Kim, W. K. Kim, B. S. Han, S. G. Park, B. H. Chung, S. C. Lee and K. H. Bae, *PLoS One*, 2014, **9**, e97747.
41 M. Zhu, E. Lanni, N. Garg, M. E. Bier and R. Jin, *J. Am. Chem. Soc.*, 2008, **130**, 1138–1139.
42 A. Gil, J. Olza, M. Gil-Campos, C. Gomez-Llorente and C. M. Aguilera, *Int. J. Pediatr. Obes.*, 2011, **6**(Suppl 1), 13–20.
43 D. Langin, *Biochim. Biophys. Acta*, 2010, **1801**, 372–376.
44 P. Seale and M. A. Lazar, *Diabetes*, 2009, **58**, 1482–1484.
45 A. Bartelt, O. T. Bruns, R. Reimer, H. Hohenberg, H. Ittrich, K. Peldschus, M. G. Kaul, U. I. Tromsdorf, H. Weller, C. Waurisch, A. Eychmüller, P. L. Gordts, F. Rinninger, K. Bruegelmann, B. Freund, P. Nielsen, M. Merkel and J. Heeren, *Nat. Med.*, 2011, **17**, 200–205.
46 B. Cannon and J. Nedergaard, *Physiol. Rev.*, 2004, **84**, 277–359.
47 D. Ricquier and F. Bouillaud, *J. Physiol.*, 2000, **529**(Pt 1), 3–10.
48 J. Wu, P. Boström, L. M. Sparks, L. Ye, J. H. Choi, A. H. Giang, M. Khandekar, K. A. Virtanen, P. Nuutila, G. Schaart, K. Huang, H. Tu, W. D. van Marken Lichtenbelt, J. Hoeks, S. Enerbäck, P. Schrauwen and B. M. Spiegelman, *Cell*, 2012, **150**, 366–376.
49 P. Seale, S. Kajimura, W. Yang, S. Chin, L. M. Rohas, M. Uldry, G. Tavernier, D. Langin and B. M. Spiegelman, *Cell Metab.*, 2007, **6**, 38–54.
50 D. V. Chartoumpekis, I. G. Habeos, P. G. Ziros, A. I. Psyrogiannis, V. E. Kyriazopoulou and A. G. Papavassiliou, *Mol. Med.*, 2011, **17**, 736–740.
51 P. Das, M. Colombo and D. Prosperi, *Colloids Surf., B*, 2019, **174**, 42–55.
52 C. S. Kumar and F. Mohammad, *Adv. Drug Delivery Rev.*, 2011, **63**, 789–808.
53 M. Soleymani, S. Khalighfard, S. Khodayari, H. Khodayari, M. R. Kalhori, M. R. Hadjighassem, Z. Shaterabadi and A. M. Alizadeh, *Sci. Rep.*, 2020, **10**, 1695.
54 E. Cedrowska, M. Pruszynski, W. Gaweda, M. Zuk, P. Krysinski, F. Bruchertseifer, A. Morgenstern, M. A. Karageorgou, P. Bouziotis and A. Bilewicz, *Molecules*, 2020, **25**, 1025.
55 M. R. Marinozzi, L. Pandolfi, M. Malatesta, M. Colombo, V. Collico, P. M. Lievens, S. Tambalo, C. Lasconi, F. Vurro, F. Boschi, S. Mannucci, A. Sbarbati, D. Prosperi and L. Calderan, *Int. J. Biochem. Cell Biol.*, 2017, **93**, 62–73.
56 R. E. Rosensweig, *J. Magn. Magn. Mater.*, 2002, **252**, 370–374.
57 M. Suto, Y. Hirota, H. Mamiya, A. Fujita, R. Kasuya, K. Tohji and B. Jeyadevan, *J. Magn. Magn. Mater.*, 2009, **321**, 1493–1496.
58 J. Carrey, B. Mehdaoui and M. Respaud, *J. Appl. Phys.*, 2011, **110**, 039921.
59 I. Chakraborty and T. Pradeep, *Chem. Rev.*, 2017, **117**, 8208–8271.
60 Z. Lin, N. Goswami, T. Xue, O. J. H. Chai, H. Xu, Y. Liu, Y. Su and J. Xie, *Adv. Funct. Mater.*, 2021, 2105662.